

# ESTIMATING NONLINEARITY USING VOLTERRA KERNELS IN FEEDBACK WITH LINEAR MODELS

Rick Lind,<sup>1</sup>  
University of Florida

Richard J. Prazenica<sup>2</sup> and Martin J. Brenner<sup>3</sup>  
NASA Dryden Flight Research Center

## Abstract

Aeroelastic dynamics must be accurately known to ensure safe and efficient flight testing. Unfortunately, most models of aircraft systems typically describe only the linear dynamics. These models are inadequate for predicting behaviors, like limit cycle oscillations, resulting from nonlinearities. This paper presents an approach to augment a linear model by identifying associated nonlinear operators. Essentially, the difference between a flight data measurement and a simulated measurement indicates the unmodeled dynamics. Volterra kernels are computed to represent the difference in measurement and, consequently, represent the unmodeled dynamics. The approach is applied to a nonlinear pitch-plunge system for which only a linear model is assumed available. The method is able to characterize errors due to incorrect parameters in the linear model and errors due to unmodeled nonlinearities of the dynamics.

## Introduction

The analysis of nonlinear aeroelasticity is a research area of increasing importance to the flight test community. The occurrence of limit cycle oscillations resulting from these nonlinear dynamics has been noted on several aircraft [5]. Indeed, these limit cycle oscillations have been noted with varying types of behaviors which may indicate varying nonlinearities affect the dynamics [3].

Aeroelastic models, despite the importance of nonlinear dynamics in physical systems, are usually generated with assumptions of linearity. These models are used to predict the onset of flight conditions at which linear instabilities occur and, potentially, indicate conditions at which limit cycles are likely to occur [4]. In general, the actual nonlinearities existing in aircraft are not well understood and subsequently can not be modeled.

<sup>1</sup>Assistant Professor, Department of Mechanical and Aerospace Engineering, 231 Aerospace Building, Gainesville FL, 32611, *rick@mae.ufl.edu*, Senior Member AIAA

<sup>2</sup>National Research Council Fellow, MS 4840, Edwards CA 93523, *chad.prazenica@dfrc.nasa.gov*, Member AIAA

<sup>3</sup>Research Engineer, Aerostructures Branch, MS 4840, Edwards CA 93523, *martin.j.brenner@nasa.gov*, Member AIAA

Current practices for flight testing reflect the lack of accuracy for modeling nonlinear aeroelasticity. Flight data is generated that measures responses of the aircraft to various types of excitation. This data is then analyzed to extract basic information, such as damping, about the aircraft dynamics which may be used to indicate the onset of instabilities. Flight data often has characteristics that indicate it was generated from nonlinear dynamics but a uniform framework does not exist for extracting all types of characteristics.

This paper presents a method to identify nonlinear dynamics from analysis of flight data. Actually, the method identifies unknown dynamics, or errors, in a linear model by subtracting simulated data from measured data. The linear and nonlinear components of the errors are then extracted. In this way, the method identifies unmodeled linear and nonlinear dynamics associated with a model as indicated by flight data.

The approach relies on a particular formulation of the model that relates the known dynamics to the unknown dynamics through a feedback relationship. This formulation has already been demonstrated as a valid representation for many types of nonlinear systems [18]. Furthermore, the basic formulation was used for the specific problem of identifying static nonlinearities using an optimization approach [17].

Identification of the unknown dynamics is accomplished using Volterra kernels. A wavelet-based approach has been developed that identifies kernels to represent a mapping between a set of input and output data. A variant of this approach has already been utilized to extract estimates of linear uncertainty for a linear model [11].

A nonlinear pitch-plunge system is used to demonstrate the approach. This system consists of a rigid wing mounted in a wind tunnel [16]. Separate models are generated to represent the linearized dynamics such that one model has the correct estimate of pitch stiffness while the other has an incorrect estimate. Volterra kernels are identified to describe the differences between measured and predicted outputs of the system. These kernels were able to demonstrate that the inaccurate model does indeed have an error in its representation of the linearized dynamics. More importantly, these kernels also show that the dynamics have a nonlinearity that is not included with either model.

## Nonlinear Aeroelasticity

The aeroelastic systems under consideration are described by the general equation of motion in Equation 1.

$$\overline{M}\ddot{x} + \overline{C}\dot{x} + \overline{K}x - \overline{F}u = \overline{N}(z) \quad (1)$$

This general formulation uses  $x \in \mathcal{R}^{n_x}$  as the modal displacement vector and  $u \in \mathcal{R}^{n_u}$  as the input vector. The dynamics are described by  $\overline{M} \in \mathcal{R}^{n_x \times n_x}$  as the equivalent mass matrix,  $\overline{C} \in \mathcal{R}^{n_x \times n_x}$  as the equivalent damping matrix,  $\overline{K} \in \mathcal{R}^{n_x \times n_x}$  as the equivalent stiffness matrix and  $\overline{F} \in \mathcal{R}^{n_x \times n_u}$  as the equivalent input matrix. Also, the element  $\overline{N} : \mathcal{R}^{n_z} \rightarrow \mathcal{R}^{n_x}$  is the equivalent nonlinearity which is a function of  $z \in \mathcal{R}^{n_z}$ .

The matrices in Equation 1 are described as equivalents to standard elements of structural dynamics. These matrices are actually formulated by combining elements of structural dynamics and aerodynamics. Such a formulation is relatively straightforward, as will be demonstrated for a pitch-plunge example, using linear algebra. Of course, the formulation requires the unsteady aerodynamics to be represented as a rational function approximation. The derivations in this paper are not explicitly dependent on any particular realization of the dynamics; therefore, the form in Equation 1 will be used for notational simplicity.

An important feature in Equation 1 is the nonlinearity represented as  $\overline{N}(z)$ . This nonlinearity is described as a function of the signal  $z$ . In this paper, the signal  $z$  is restricted to being a linear combination of the states and inputs. The use of  $z$  allows the general formulation as presented to account for many types of nonlinearities, such as nonlinear stiffness or surface free play, using the same framework. Define this signal using  $Z_x \in \mathcal{R}^{n_z \times n_x}$  and  $Z_u \in \mathcal{R}^{n_z \times n_u}$ .

$$z = Z_x x + Z_u u \quad (2)$$

Finally, a set of measurements are available from flight testing of the aeroelastic system. Define these sensor measurements,  $\overline{y}$ , using  $Y_x \in \mathcal{R}^{n_y \times n_x}$  and  $Y_u \in \mathcal{R}^{n_y \times n_u}$ .

$$\overline{y} = Y_x x + Y_u u \quad (3)$$

The formulation of Equation 1 is assumed to be an accurate representation of the dynamics of a system. Any physical system will not be exactly described by such a simple formulation; however, the formulation is reasonably accurate for many systems of interest.

### Model

A model of the aeroelastic system in Equation 1 is developed also using the concepts of equivalent matrices. The equation of motion for this model is given in Equation 4.

$$M\ddot{x} + C\dot{x} + Kx - Fu = X(z) \quad (4)$$

This model is assumed to contain the same number of modal displacements and inputs as the true system in Equation 1. Namely,  $x \in \mathcal{R}^{n_x}$  and  $u \in \mathcal{R}^{n_u}$  are dimensioned such  $M \in \mathcal{R}^{n_x \times n_x}$ ,  $C \in \mathcal{R}^{n_x \times n_x}$ ,  $K \in \mathcal{R}^{n_x \times n_x}$  and  $F \in \mathcal{R}^{n_x \times n_u}$ . The additional signal  $z \in \mathcal{R}^{n_z}$  is dimensioned such that the remaining term,  $X : \mathcal{R}^{n_z} \rightarrow \mathcal{R}^{n_x}$ , is a mapping of appropriate dimension.

The function,  $X(z)$ , represents an unknown, possibly nonlinear, contribution to the dynamics. This mapping is simply represented in a fashion analogous to the nonlinearity of the true dynamics; namely, the unknown dynamics are a function of the states and inputs whose linear combination is described by  $z$ .

The known and unknown elements of the model can be related through feedback by introducing a signal  $w \in \mathcal{R}^{n_x}$ .

$$w = X(z) \quad (5)$$

The inclusion of  $w$  allows the unknown element,  $X(z)$ , to be removed from the equation of motion and replaced by a feedback relationship. Instead, the system dynamics are now represented by a set of equations. These equations, along with the formulations for the sensor measurements,  $y$ , and functional dependency,  $z$ , are given in Equation 6.

$$\left\{ \begin{array}{l} \ddot{x} = -M^{-1}Kx - M^{-1}C\dot{x} + M^{-1}Fu + M^{-1}w \\ y = Y_x x + Y_u u \\ z = Z_x x + Z_u u \end{array} \right\} \quad (6)$$

A single model,  $P$ , is developed to represent the dynamics described in these equations. The inputs to the model are the signals  $u$  and  $w$  whereas the outputs from the model are the signals  $y$  and  $z$ . This model can be realized as a state-space system because the known dynamics are assumed to be linear.

$$P = \left[ \begin{array}{cc|cc} 0 & I & 0 & 0 \\ -M^{-1}K & -M^{-1}C & M^{-1}F & M^{-1} \\ \hline Y_x & 0 & Y_u & 0 \\ Z_x & 0 & Z_u & 0 \end{array} \right]$$

The model,  $P$ , is related to the unknown dynamics,  $X(z)$ , through a feedback relationship as shown in Figure 1.

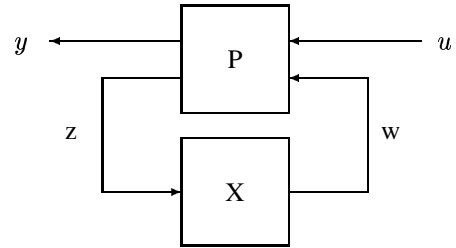


**Figure 1:** Feedback Relationship of Operators

## Operator Identification

The system as represented in Figure 1 has a natural decomposition that separates known and unknown elements. As such, the identification of the unknown operator is straightforward. This approach allows maximum usage of the known dynamics of the system for estimating the unknown dynamics.

The derivation of the identification procedure is simplified by considering a particular representation of  $P$ . This model was originally presented in terms of a state-space matrix quadruple; however, it can also be presented as a matrix of transfer functions. In this case,  $P$  is described as matrix of 4 transfer functions relating the 2 inputs to the 2 outputs.

$$P = \begin{bmatrix} P_{11} & P_{12} \\ P_{21} & P_{22} \end{bmatrix} \quad (7)$$

The unknown operator,  $X(z)$ , can be identified as a mapping between the  $z$  and  $w$  signals. As such, these signals must be isolated. Such an isolation can be accomplished using the elements,  $P_{11}$  and  $P_{12}$ , of the transfer function matrix. These elements are used to compute the expected output measurements of the model by noting that  $w = X(z)$ .

$$y = P_{11}x + P_{12}X(z) \quad (8)$$

The operator is chosen such that the expected output of the model,  $y$ , matches the measurements from the system,  $\bar{y}$ , acquired by flight data. Consequently, the unknown element can be identified as an optimization.

$$X = \arg \min_f \|\bar{y} - P_{11}x - P_{12}f(z)\| \quad (9)$$

This formulation in Equation 9 is a particularly attractive approach for flight test programs. Essentially, the minimization is based on the difference between measured and simulated data. The measurement data,  $\bar{y}$ , represents the nonlinear system and the simulated data,  $P_{11}x$ , represents the linearized model.

A representation for  $X(z)$  can be computed as a set of Volterra kernels. These kernels allow linear and nonlinear elements of the unknown dynamics to be identified. Of course, several techniques for system identification can be applied but this paper will restrict attention to Volterra kernels.

## Volterra Kernels

Volterra series representations provide a convenient framework for the analysis of nonlinear dynamical systems. The Volterra theory of nonlinear systems states that the system output,  $w$ , can be expressed in terms of an infinite series of integral operators of increasing order [13, 14].

$$w(t) = w_1(t) + w_2(t) + w_3(t) + \dots + w_\infty(t) \quad (10)$$

In practice, the series is truncated and this paper considers Volterra models that include only the first, second, and third-order operators. For a causal, time-invariant, single-input/single-output system, these operators take the form

$$w_1(t) = \int_0^t h_1(\xi)z(t-\xi)d\xi \quad (11)$$

$$w_2(t) = \int_0^t \int_0^t h_2(\xi, \eta)z(t-\xi)z(t-\eta)d\xi d\eta \quad (12)$$

$$w_3(t) = \int_0^t \int_0^t \int_0^t h_3(\xi, \eta, \gamma)z(t-\xi)z(t-\eta)z(t-\gamma)d\xi d\eta d\gamma \quad (13)$$

where  $z$  is the input and  $h_1, h_2, h_3$  denote the first, second, and third-order Volterra kernels. Collectively, the Volterra kernels provide a model of the system since, once the kernels have been identified, the response to any arbitrary input can be determined. The first-order kernel represents the linear dynamics of the system while the higher-order kernels characterize the nonlinear dynamics. It should be noted that, for a linear system, the first-order kernel is equivalent to the impulse response of the system and the output is given by Equation 11. Therefore, the Volterra theory can be viewed as an extension of the concept of linear convolution to nonlinear systems.

Boyd and Chua [2] have demonstrated that, in general, any system that exhibits fading memory can be approximated to arbitrary accuracy in terms of a truncated Volterra series. Fading memory asserts that past inputs have a diminishing influence on the present output. This implies that all of the Volterra kernels of a given system decay to zero in a finite period of time. Many systems in engineering practice satisfy this requirement; therefore, the Volterra theory is applicable to a large class of dynamical systems. The truncation error associated with a finite Volterra series representation is related to the input amplitude [2]. This paper considers Volterra series that have been truncated to include only the first, second, and third-order operators. For many systems of interest, it has been demonstrated that the second and third-order kernels are sufficient to characterize the nonlinear dynamics when the input amplitude is sufficiently bounded.

The identification of Volterra kernels is a difficult problem in practice. By nature, it is an ill-posed, inverse problem since the system model, in the form of Volterra kernels, must be determined from input/output measurements from the system. Typically, a large number of parameters are needed to represent the kernels, with the number increasing geometrically with the order of the kernel. A diverse range of approaches have been taken to identify Volterra kernels in both the time and frequency domains. The harmonic probing method [1] is commonly used to measure kernels in the frequency domain. Time-domain approaches include the application of discrete impulse inputs [15], variations of the cross-correlation technique [8], and expanding the kernels in terms of a set of basis functions such as decaying exponentials [12].

The approach taken in this paper is to represent first, second, and third-order kernels in terms of a multiwavelet basis. Wavelets are compactly-supported, oscillatory functions that are constructed to satisfy certain properties such as orthogonality, smoothness, and symmetry requirements. Multiwavelets are composed of a set of wavelet functions  $\{\psi^1, \dots, \psi^r\}$  that are generated from a set of scaling functions  $\{\phi^1, \dots, \phi^r\}$  [6]. The scaled translates and dilates of the multiwavelets form a basis for  $L^2(\mathcal{R})$ , the space of square-integrable functions. Higher-dimensional multiwavelets are easily constructed as tensor products of the one-dimensional scaling functions and multiwavelets. The main motivation for using wavelet expansions is that they provide information about the kernels in both the time and frequency domains. Often, many of the wavelet coefficients are very small and can be neglected, leading to reduced-order representations of the kernels.

This paper employs piecewise-quadratic multiwavelets that have been constructed using the technique of intertwining [6]. This process derives four scaling functions and associated multiwavelets from the classical quadratic finite element basis functions. The details of this construction and plots of the multiwavelets are given in Ref. [10]. This class of multiwavelets is well-suited for the approximation of Volterra kernels because the functions are orthogonal, symmetric or anti-symmetric, and are easily adapted to the finite domains over which the kernels are supported.

Multiwavelet expansions of the kernels are substituted into Equations 11 through 13 along with a zero-order hold, or piecewise-constant, approximation of the input. Then, the kernel identification problem reduces to a matrix equation of the form

$$\underline{w}_j = [A_1 \ A_2 \ A_3] \begin{Bmatrix} \underline{\beta}_1 \\ \underline{\beta}_2 \\ \underline{\beta}_3 \end{Bmatrix} \quad (14)$$

In Equation 14,  $\underline{w}_j$  represents a vector of discrete outputs that have been sampled at  $2^j$  Hz. The vectors  $\underline{\beta}_1, \underline{\beta}_2, \underline{\beta}_3$  are composed of the multiscale wavelet coefficients that represent the first, second, and third-order kernels. It should be noted that the formulation in Equation 14 takes into account the fact that the Volterra kernels can be assumed to be symmetric [14]. This reduces the number of second and third-order coefficients in the model by roughly factors of two and six, respectively. Equation 14 is solved, in a least-squares sense, for the first, second, and third-order kernel coefficients. In many cases, the vectors  $\underline{\beta}_1, \underline{\beta}_2, \underline{\beta}_3$  can be truncated to obtain reduced-order representations of the kernels.

### Specific Formulations

#### Concept

The model presented in Figure 1 is a general formulation that can be used to represent a broad range of systems. This gen-

eral formulation can often be recast for specific models. In particular, the models can be altered if the unknown dynamics are assumed to be functions of either the states or the inputs.

Specific formulations are derived for two different models. One model assumes the unknown dynamics are purely a function of the states. Another model assumes the unknown dynamics are purely a function of the inputs. These formulations are presented to demonstrate that the generalized formulation in Figure 1 does indeed converge to formulations common to specific types of models.

#### Unknown Function of State

Consider a formulation that assumes the unknown dynamics are functions of the states. Such an assumption implies that  $z = x$  and, consequently,  $X(z) = X(x)$ . The open-loop model can thus be written to reflect this specific formulation.

$$P = \left[ \begin{array}{cc|cc} 0 & I & 0 & 0 \\ -M^{-1}K & -M^{-1}C & M^{-1}F & M^{-1} \\ \hline I & 0 & 0 & 0 \\ I & 0 & 0 & 0 \end{array} \right] \quad (15)$$

This model can also be expressed as the matrix of transfer functions. Noting the relationship between each input and output allows the system to be written as in Equation 16.

$$P = \begin{bmatrix} P_{11} & P_{12} \\ P_{11} & P_{12} \end{bmatrix} \quad (16)$$

Obviously the model has a redundancy in that both outputs are identical. As such, the system could be simplified from the general representation in Figure 1 to the reduced representation in Figure 2.

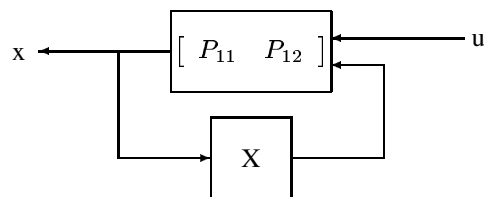


**Figure 2:** Model with Unknown Function of States

This graphical representation demonstrates an important feature of the measured data. Namely, the measurements,  $x$ , are affected by a nonlinearity that is itself a function of  $x$ . Thus, the dynamics inherently have a feedback relationship that is easily symbolized using the general representation in Figure 1 or specific representation in Figure 2.

#### Unknown Function of Input

Consider a formulation that assumes the unknown dynamics are a function of the input. Such an assumption implies that  $z = u$  and, consequently,  $X(z) = X(u)$ . The open-loop

model can thus be written to reflect this specific formulation.

$$P = \left[ \begin{array}{cc|cc} 0 & I & 0 & 0 \\ -M^{-1}K & -M^{-1}C & M^{-1}F & M^{-1} \\ \hline I & 0 & 0 & 0 \\ 0 & 0 & I & 0 \end{array} \right] \quad (17)$$

A matrix of transfer functions is again a convenient representation for this model. Such a representation is given in Equation 18.

$$P = \left[ \begin{array}{cc} P_{11} & P_{12} \\ I & 0 \end{array} \right] \quad (18)$$

This formulation indicates the second output of the system, as expected, is simply the first input of the system. The system can thus be greatly simplified from the general block diagram of Figure 1 to the reduced block diagram in Figure 3.

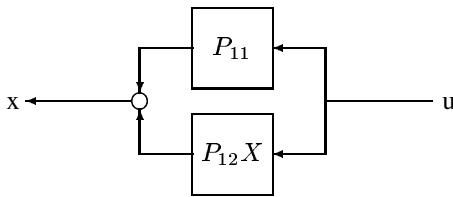


**Figure 3:** Model with Unknown Function of Inputs

This graphical representation is particularly relevant to the use of Volterra kernels. Specifically, the Volterra kernels assume the measurement can be separated into a linear and nonlinear component. The block diagram in Figure 3 clearly shows the measurement,  $x$ , is simply the added outputs of a linear system and an unknown system. Allowing the unknown system to include the nonlinearity allows Figure 3 to exactly match the assumptions associated with Volterra modeling.

### Interpreting Unknown Element

The formulation of a linear model will always have some errors. An obvious source of error is the omission of the nonlinear dynamics but another source of error is incorrect estimates of the linearized dynamics. The unknown element,  $X(x)$ , is Equation 4 can be interpreted in terms of these errors.

Consider a particular situation in which the linearized component of the structural dynamics is modeled accurately except for the stiffness. Introduce a term,  $\Delta_K \in \mathcal{R}^{n_x \times n_x}$ , to represent the error in the linearized stiffness of the model. Essentially, relate the terms in the model of Equation 4 to the terms in the system dynamics of Equation 1 using the simple relationships in Equations 19-22.

$$M = \bar{M} \quad (19)$$

$$C = \bar{C} \quad (20)$$

$$K = \bar{K} + \Delta_K \quad (21)$$

$$F = \bar{F} \quad (22)$$

The model is thus described as in Equation 23.

$$\bar{M}\ddot{x} + \bar{C}\dot{x} + (\bar{K} + \Delta_K)x - \bar{F}u = X(z) \quad (23)$$

The model in Equation 23 is equivalent to the system dynamics in Equation 1 for a special case of the unknown dynamics given in Equation 24.

$$X(z) = N(z) + \Delta_K x \quad (24)$$

The meaning of the unknown dynamics is clear in this case. Specifically, the term,  $X(z)$ , represents the error caused by unmodeled nonlinear dynamics and the error caused by inaccurate linear dynamics. The formulation in Equation 24 considers error in stiffness but the derivation is easily extended to consider error in mass and damping also.

## Example

### Pitch-Plunge System

The process of estimating a model to describe aeroelastic dynamics is applied to a pitch-plunge system. This system is comprised of a rigid airfoil, whose motion is restricted to pitching and plunging, mounted in a wind tunnel at Texas A&M University.

The dynamics of the system are described to within a high degree of accuracy by Equation 25.

$$\begin{aligned} & \rho U^2 b s \begin{bmatrix} -c_{l_\alpha} \left( \alpha + \frac{1}{U} \dot{h} + \left( \frac{1}{2} - a \right) b \frac{1}{U} \dot{\alpha} \right) + c_{l_\beta} \beta \\ c_{m_\alpha} \left( \alpha + \frac{1}{U} \dot{h} + \left( \frac{1}{2} - a \right) b \frac{1}{U} \dot{\alpha} \right) + c_{m_\beta} \beta \end{bmatrix} \\ &= \begin{bmatrix} m_T & m_w x_\alpha b \\ m_w x_\alpha b & I_\alpha \end{bmatrix} \begin{bmatrix} \ddot{h} \\ \ddot{\alpha} \end{bmatrix} \\ &+ \begin{bmatrix} c_h & 0 \\ 0 & c_\alpha \end{bmatrix} \begin{bmatrix} \dot{h} \\ \dot{\alpha} \end{bmatrix} + \begin{bmatrix} k_h & 0 \\ 0 & k_\alpha \end{bmatrix} \begin{bmatrix} h \\ \alpha \end{bmatrix} \\ &+ \begin{bmatrix} 0 \\ k_{\alpha^2} \alpha^2 \end{bmatrix} \end{aligned} \quad (25)$$

These dynamics describe the complete aeroelastic system. The degrees of freedom of the rigid airfoil are described by the plunge,  $h$ , and the pitch,  $\alpha$ , parameters. The left side of the equality describes the quasi-steady aerodynamics that are generated in response to motion of the airfoil and commanded rotations,  $\beta$ , of a flap. The right side of the equality describes the structural dynamics.

The system has been constructed to include a nonlinearity in the structural dynamics. Specifically, the stiffness affecting pitch motion is a nonlinear function of the pitch angle. The dynamics used in this paper consider a quadratic nonlinearity for this stiffness term.

The parameters describing the dynamics of the system are given in Table 1. These parameters are generally indicative

of those presented in several references [7, 9]; however, the value of pitch damping has been increased simply to ensure the identified kernels decay within 4 *sec* for ease of computation.

parameter	parameter
$U = 6 \text{ m/s}$	$a = -0.6$
$b = 0.135 \text{ m}$	$\rho = 1.225 \text{ kg/m}^3$
$m = 12.387 \text{ kg}$	$x_\alpha = 0.2466$
$I_\alpha = 0.065 \text{ m}^2 \text{ kg}$	$k_h = 2844.4 \text{ N/m}$
$c_\alpha = 0.180 \text{ m}^2 \text{ kg/s}$	$c_h = 27.43 \text{ kg/s}$
$c_{l_\alpha} = 6.28$	$c_{m_\alpha} = -0.628$
$c_{l_\beta} = 3.358$	$c_{m_\beta} = -0.635$
$k_\alpha = 2.82$	$k_{\alpha^2} = 14.1$

**Table 1:** System Parameters

### Model Formulation

Models of the aeroelastic system are developed from the theoretical equations of motion. This model has the exact form of the linearized dynamics in Equation 25. Essentially, the model contains all of Equation 25 excepting the nonlinear contribution of  $k_{\alpha^2} \alpha^2$  to the moment.

The model is formulated using the equivalent matrices as in Equation 4. These equivalent matrices are straightforward to derive by combining terms in  $[y, \alpha]$  and  $[\dot{y}, \dot{\alpha}]$ .

$$M = \begin{bmatrix} m_T & m_w x_\alpha b \\ m_w x_\alpha b & I_\alpha \end{bmatrix}$$

$$C = \left( \begin{bmatrix} c_h & 0 \\ 0 & c_\alpha \end{bmatrix} - \rho b s U \begin{bmatrix} -c_{l_\alpha} & -(\frac{1}{2} - a) b c_{l_\alpha} \\ b c_{m_\alpha} & (\frac{1}{2} - a) b^2 c_{m_\alpha} \end{bmatrix} \right)$$

$$K = \left( \begin{bmatrix} k_h & 0 \\ 0 & k_1 \end{bmatrix} - \begin{bmatrix} 0 & -\rho U^2 b s c_{l_\alpha} \\ 0 & \rho U^2 b^2 s c_{m_\alpha} \end{bmatrix} \right)$$

$$F = \begin{bmatrix} -\rho U^2 b s c_{l_\beta} \\ \rho U^2 b^2 s c_{m_\beta} \end{bmatrix}$$

Also, a sensor is included that allows pitch angle to be measured. Define the standard basic vector,  $e_2^T = [0 \ 1]$ , such that  $y = [y \ \alpha] e_2$  represents this measurement.

A state-space plant model,  $P$ , is thus created.

$$P = \left[ \begin{array}{cc|cc} 0 & I & 0 & 0 \\ -M^{-1}K & -M^{-1}C & M^{-1}F & M^{-1}e_2 \\ \hline e_2^T & 0 & 0 & 0 \\ e_2^T & 0 & 1 & 0 \end{array} \right]$$

The model,  $P$ , is related to the unknown dynamics,  $X$ , through a feedback relationship as shown in Figure 1.

A pair of models are developed to describe the linearized dynamics using the values from Table 1. The only difference between these models is the value of the pitch stiffness. One model is formulated using the correct value of pitch stiffness

model	$k_\alpha$
accurate	2.82
inaccurate	2.26

**Table 2:** Model Parameters

while the other model is formulated using an incorrect value of pitch stiffness as shown in Table 2.

The unknown dynamics associated with these models are computed using separate approaches. The first approach will consider the unknown dynamics as a function of pitch angle while the second approach will consider the unknown dynamics as a function of input flap command.

### Estimating $X(x)$ with Accurate Linear Model

The procedure discussed in this paper is used to estimate the unknown dynamics associated with a linear model of the system. This linear model is formulated as an accurate representation of the linearized dynamics of the pitch-plunge aeroelastic system. Thus, the estimation of the unknown dynamics are actually an estimation of the nonlinearity in the dynamics.

Response data is simulated from the nonlinear dynamics by commanding a chirp signal to the flap. This chirp command ranges from 0.0 to 5.0 *Hz* over 32 *sec*. The magnitude of the flap command is 10 *deg*.

The pitch angle simulated in response to this chirp signal is shown in Figure 4 for the nonlinear dynamics and the linear model. Clearly these responses differ indicating the chirp command is exciting the nonlinearity. Consequently, the response of the nonlinear dynamics should contain sufficient information to allow estimation of the nonlinearity.

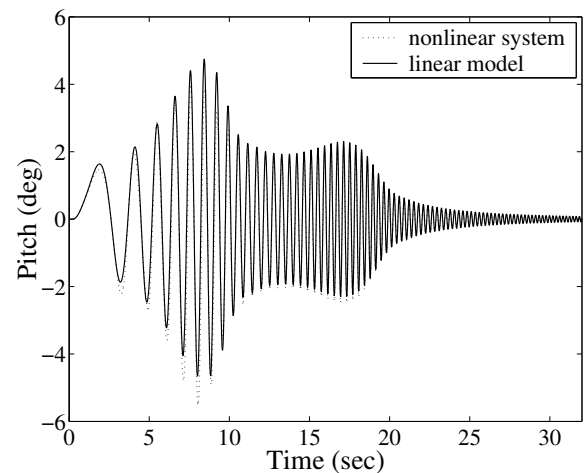


**Figure 4:** Response of Nonlinear Dynamics and Linear Model

The difference between measured data from the nonlinear system and simulated data from the linearized model is used to identify the unknown dynamics. Essentially, the Volterra kernels attempt to represent the dynamics that may have gen-

erated this difference. The approach using wavelets is used to generate the kernels. The resulting signal is shown to compare quite closely with the computed difference between linear and nonlinear responses as shown in Figure 5.

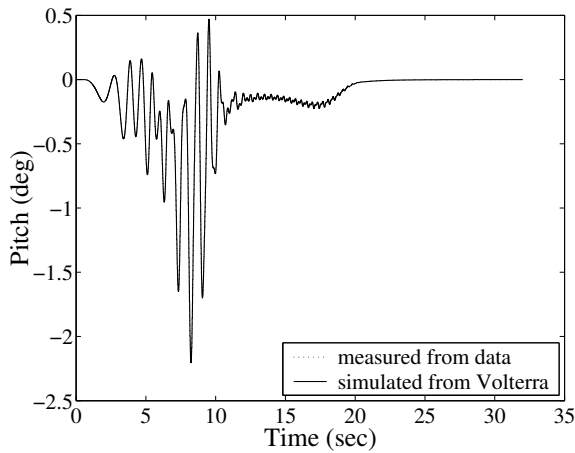


**Figure 5:** Difference in Measurements from Nonlinear Dynamics and Linear Model

The unknown dynamics associated with the linearized model are represented by the first-order kernel in Figure 6 and the second-order kernel in Figure 7.

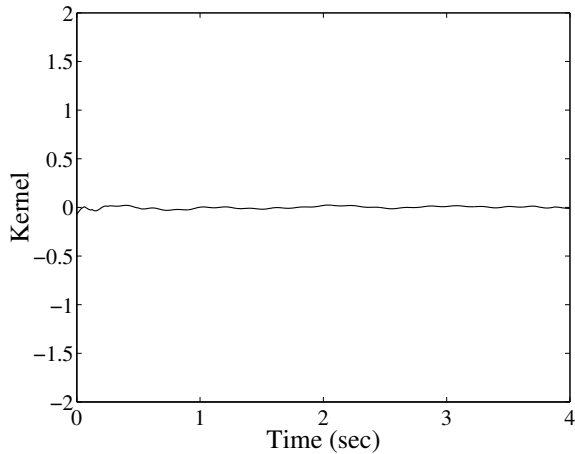


**Figure 6:** Estimated First-Order Volterra Kernel

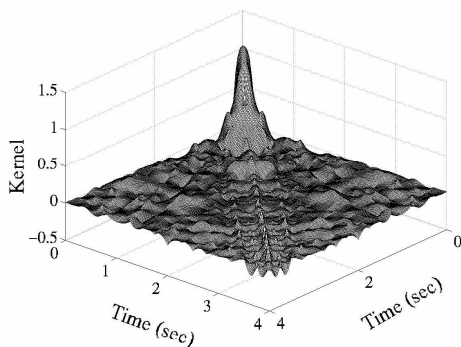


**Figure 7:** Estimated Second-Order Volterra Kernel

These kernels demonstrate the validity of the estimation process. Consider that the model as formulated included an accurate representation of the linear dynamics but did not include any nonlinearities. Accordingly, the first-order kernel, which represents the linear components of the unknown dynamics, is small while the second-order kernel, which represents the nonlinear component of the unknown dynamics, is large. The small size of the first-order kernel indicates that no linear dynamics are unknown so indeed the model must contain the accurate linearized dynamics. The large size of the second-order kernel indicates that the system definitely includes a nonlinearity which is not contained in the model. Both of these statements agree with the model formulation.

Another demonstration of the validity of the estimation process is to generate responses from the identified model. Estimates of pitch angle are generated in response to a chirp command to the linear model with the Volterra kernels in feedback. These estimated responses are shown with the original simulated responses in Figure 8. Clearly the nonlinear model is able to reproduce this response of the nonlinear dynamics.

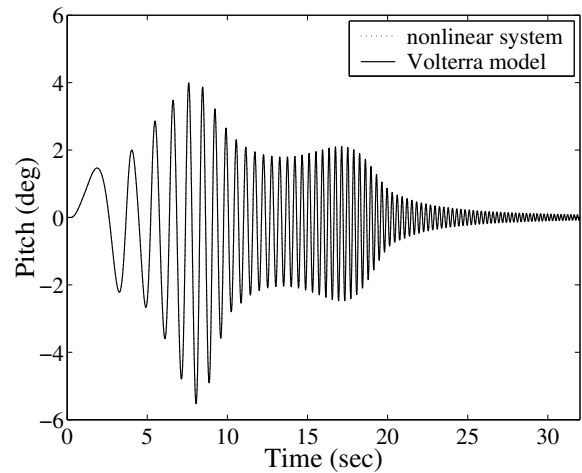


**Figure 8:** Response of Nonlinear Dynamics and Nonlinear Model

### Estimating $X(x)$ with Inaccurate Linear Model

The procedure is also applied to compute the unknown dynamics associated with an inaccurate linearized model. As mentioned, the linearized model is computed using an incorrect value of pitch stiffness. Thus, the unknown dynamics are actually representative of the unmodeled nonlinearity and the error in pitch stiffness.

The responses of the nonlinear system and the linearized model to chirp inputs are shown in Figure 9. The response of the nonlinear system is identical to that in Figure 4 but the response of the linearized model is different. That difference is caused by the change in pitch stiffness for the linearized model.

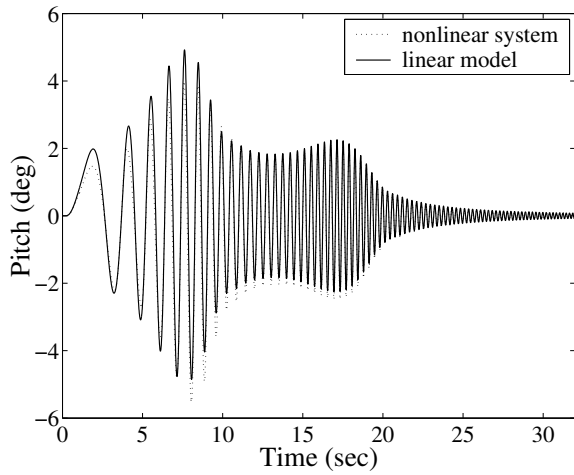


**Figure 9:** Response of Nonlinear Dynamics and Linear Model

Volterra kernels are computed to represent the dynamics associated with the difference between the responses in Figure 9. As shown in Figure 10, these kernels are able to match the difference in response as a function of the pitch angle.

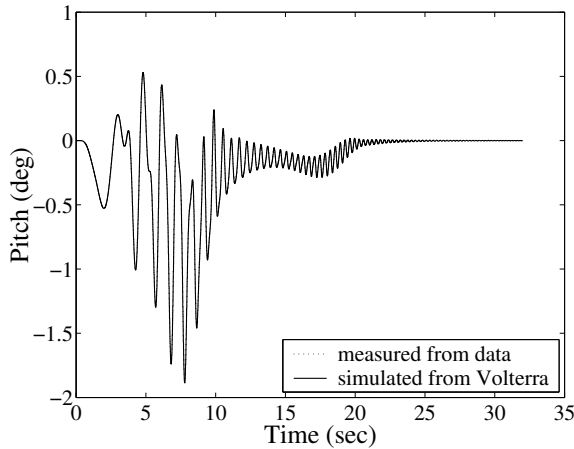


**Figure 10:** Difference in Measurements from Nonlinear Dynamics and Linear Model

The Volterra kernels identified from the response difference are shown in Figure 11 and Figure 12. Again, these kernels represent the first-order and second-order dynamics.

These kernels are demonstrative of the capabilities of the approach. Note particularly the differences between the first-order kernel in Figure 6 and the first-order kernel in Figure 11. The kernel in Figure 6 is small to indicate the linearized model matches the linearized dynamics of the system. Conversely, the kernel in Figure 11 is large and indicates the linearized model does not match the linearized dynamics of the system. Thus, the approach is able to compute unknown dynamics that account for both errors in unmodeled nonlinearities and errors in inaccurate linearization.

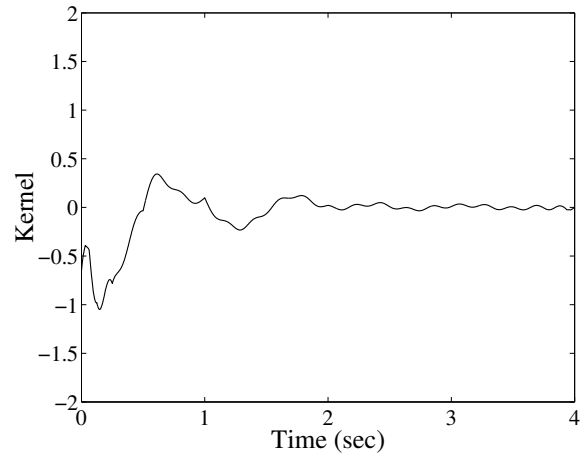


**Figure 11:** Estimated First-Order Volterra Kernel

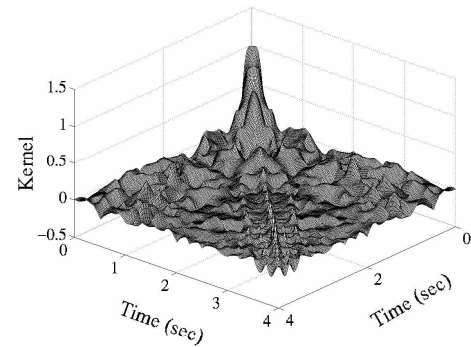


**Figure 12:** Estimated Second-Order Volterra Kernel

### Estimating $X(u)$ with Accurate Linear Model

An estimate of the unknown dynamics is again computed for the linear model; however, these unknown dynamics are now considered as a function of the input.

Data is generated in response to summation of several chirp signals between 0 and 4 Hz. The difference in responses, as shown in Figure 13, is reproduced by Volterra kernels.

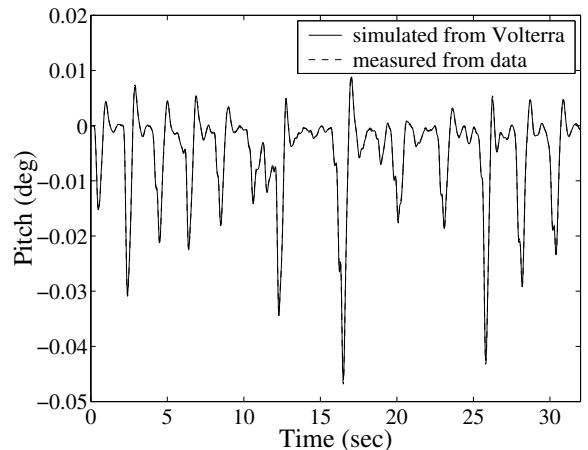


**Figure 13:** Difference in Measurements from Nonlinear Dynamics and Accurate Linear Model

The dynamics which generated the difference in Figure 13 are identified as first-order, second-order and third-order kernels. These kernels are shown in Figures 14 - 16. Note that, since the third-order kernel exists over a three-dimensional domain, only one slice of the kernel at  $\gamma = .5 \text{ sec}$  is shown in Figure 16.

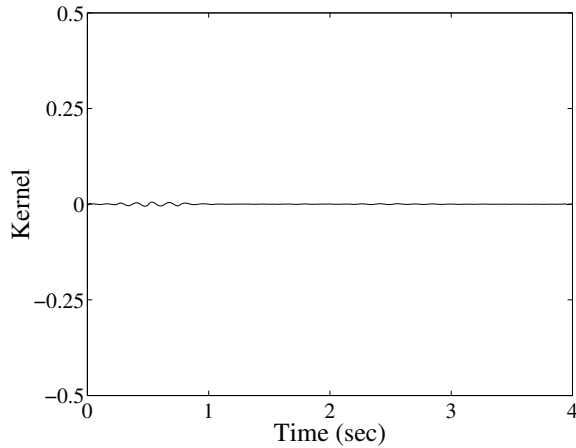


**Figure 14:** Estimated First-Order Volterra Kernel

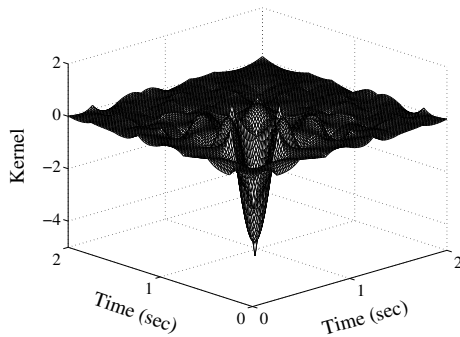


**Figure 15:** Estimated Second-Order Volterra Kernel

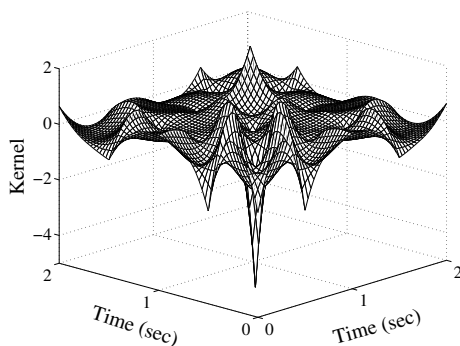


**Figure 16:** Slice of Estimated Third-Order Volterra Kernel

From Figure 14, the first-order kernel is essentially zero, indicating that there are no unmodeled linear dynamics. This is consistent with the assumption that the linear model is accurate. The second and third-order kernels, on the other hand, are not zero and represent a model of the system nonlinearity.

Clearly, these kernels are capable of predicting the nonlinear component of the response that cannot be accounted for in the linear model.

Also, these kernels are quite smooth. This feature results from an advantageous choice of input signal. Essentially, the multichirp input, composed of several chirps summed together, is able to provide better excitation than a single chirp. Thus, the kernels in Figure 14-16 seem geometrically smoother than those in Figure 11-12.

### Estimating $X(u)$ with Inaccurate Linear Model

In this example, Volterra kernels are now used to estimate the unknown dynamics associated with an inaccurate linear model. Once again, these dynamics are modeled in terms of functionals of the input flap deflection. Since the linear model is now assumed to be inaccurate, the unknown dynamics are due to both the nonlinearity in the system and error in the linear model.

Response data is simulated by using the same input signal as in the previous example. The unknown dynamics in this case are obtained as the difference between the simulated response and the response predicted by the inaccurate linear model. Once again, first, second, and third-order kernels are identified from the unknown dynamics. The response predicted by the identified kernels is compared to the the unknown dynamics in Figure 17. From the figure, it is clear that the kernels accurately reproduce these dynamics.

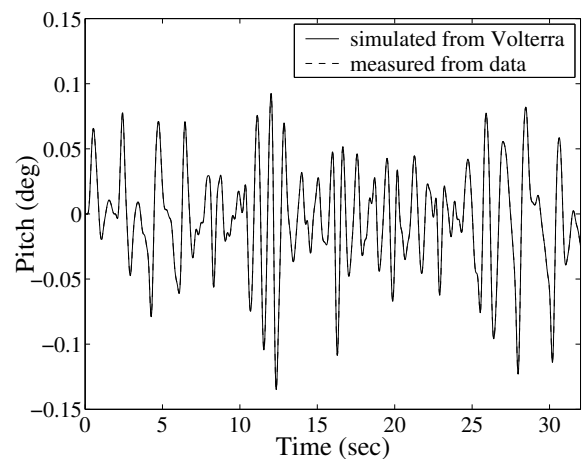


**Figure 17:** Difference in Measurements from Nonlinear Dynamics and Inaccurate Linear Model

The identified kernels are shown in Figures 18 - 20. The first-order kernel in Figure 18 is no longer zero, indicating that there is a linear component in the unknown dynamics. This is, of course, due to the error in the linear model. The response predicted by the first-order kernel is compared to the error in the linear model in Figure 21. Clearly, the first-order kernel is able to account for the error in the linear model.

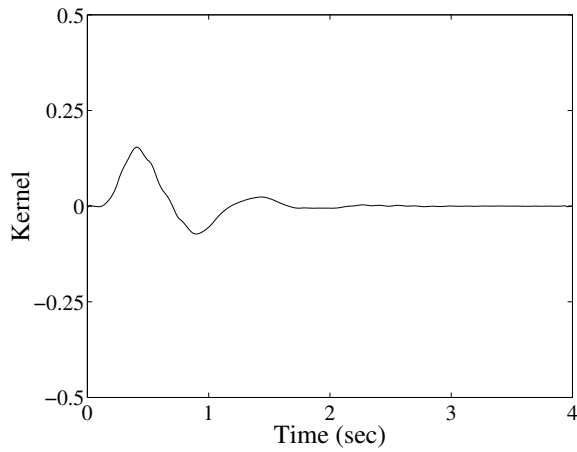


**Figure 18:** Estimated First-Order Volterra Kernel

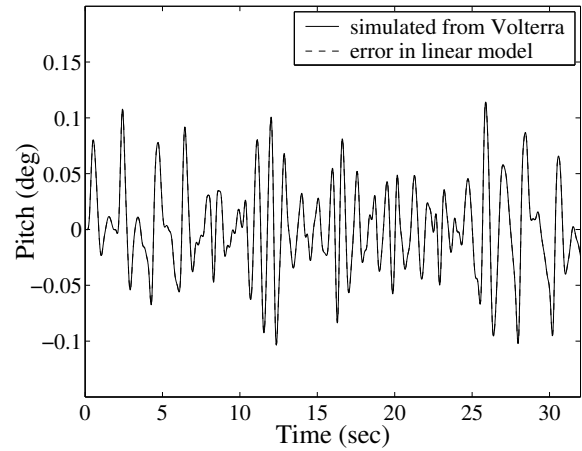


**Figure 21:** Simulated Response from First-Order Volterra Kernel

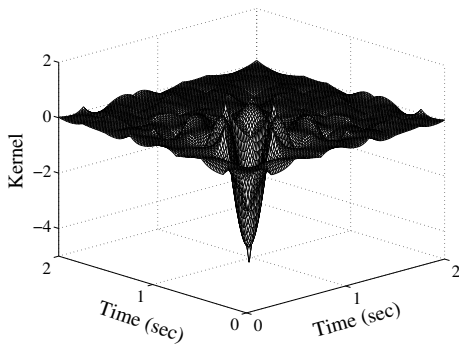


**Figure 19:** Estimated Second-Order Volterra Kernel

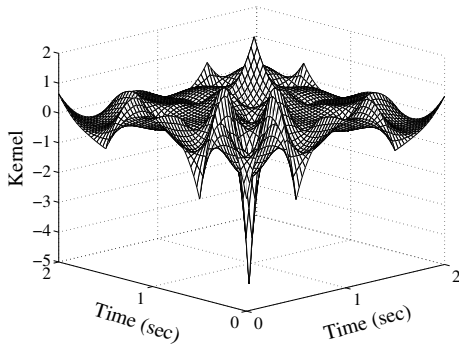


**Figure 20:** Slice of Estimated Third-Order Volterra Kernel

The identified second and third-order kernels are virtually identical to those obtained in the previous example. This is expected since the nonlinear component of the response did not change in this example. Collectively, then, the identified Volterra kernels are able to account for both error in the linear model as well as the unmodeled nonlinear component of the dynamics.

### Validation of Volterra Kernels

An important consideration in identifying Volterra kernels is to verify that the kernels are an accurate representation of the system and not merely a curve-fit of the training data. The kernels can be validated by evaluating their ability to predict the response of the system to novel inputs. The kernels identified in the previous examples were validated using several novel data sets. One such example is shown in Figures 22 and 23 for a sine input of frequency 1 Hz and amplitude 5.7 deg. In this example, the ability of the identified second and third-order kernels to model the nonlinear component of the response is examined. The response predicted by the second-order kernel is shown in Figure 22 while the total response predicted by both the second and third-order kernels is shown in Figure 23.

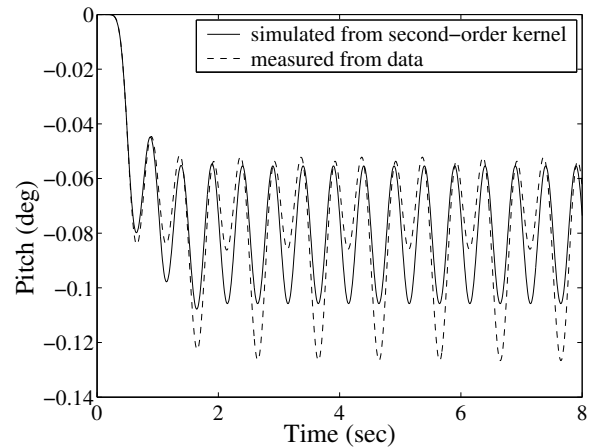


**Figure 22:** Nonlinear Component of Response Predicted by the Second-Order Kernel

Several observations can be made from these plots. First, the kernels are capable of reproducing the nonlinear component of the response. Although only a coarse representation of the third-order kernel was identified, it still provides a noticeable improvement in the prediction over the second-order

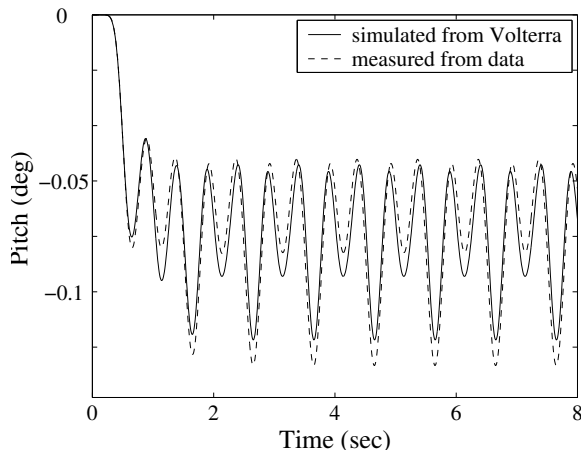


**Figure 23:** Nonlinear Component of Response Predicted by the Second and Third-Order Kernels

kernel alone. Errors in the prediction are due to errors in the identified kernels as well as contributions from the kernels of fourth-order and higher, which are not included in the model. In general, the truncation error in the Volterra series grows with the input amplitude. Therefore, the identified Volterra model is valid provided that the input amplitude is sufficiently bounded.

### Conclusion

This paper presents a method for identifying the unknown dynamics, or errors, in a linear model. These errors generally include errors due to incorrect parameters for the linearized dynamics and unmodeled parameters for the nonlinearized dynamics. The approach considers a general formulation that relates a linearized model to the unknown dynamics through a feedback relationship. These unknown dynamics are then identified as a set of Volterra kernels. The approach is applied to a nonlinear aeroelastic system by considering both accurate and inaccurate models of the linearized dynamics. The unknown dynamics are identified and, in each case, demonstrate any errors in the linearized dynamics and the unmodeled nonlinearities in the system.

### **References**

[1] Bedrosian, E. and Rice, S.O., "The Output Properties of Volterra Systems (Nonlinear Systems with Memory) Driven By Harmonic and Gaussian Inputs," *Proceedings of the IEEE*, Vol. 59, No. 12, 1971, pp. 1688-1707.

[2] Boyd, S. and Chua, L.O., "Fading Memory and the Problem of Approximating Nonlinear Operators with Volterra Series," *IEEE Transactions on Circuits and Systems*, Vol. CAS-32, No. 11, 1985, pp. 1150-1161.

[3] Buntun, R.W. and Denegri, C.M., "Limit Cycle Oscillation Characteristics of Fighter Aircraft," *Journal of Aircraft*, Vol. 37, No. 5, September-October 2000, pp. 916-918.

[4] Chen, P.C., Sarhaddi, D. and Liu, D.D., "Limit Cycle Oscillation Studies of a Fighter with External Stores," AIAA-98-1727.

[5] Denegri, C.M., "Limit Cycle Oscillation Flight Test Results of a Fighter with External Stores," *Journal of Aircraft*, Vol. 37, No. 5, September-October 2000, pp. 761-769.

[6] Donovan, G., Geronimo, J., and Hardin, D., "Intertwining Multiresolution Analyses and the Construction of Piecewise-Polynomial Wavelets", *SIAM Journal of Mathematical Analysis*, Vol. 27, No. 6, Nov 1996, pp. 1791-1815.

[7] Ko, J., Strganac, T.W. and Kurdila, A.J., "Stability and Control of a Structurally Nonlinear Aeroelastic System," *Journal of Guidance, Control, and Dynamics*, Vol. 21, No. 5, September-October 1998, pp. 718-725.

[8] Lee, Y.W. and Schetzen, M., "Measuring of the Wiener Kernels of a Non-Linear System by Cross-Correlation," *International Journal of Control*, Vol. 2, No. 3, 1965, pp. 237-254.

[9] O'Neil, T. and Strganac, T.W., "Aeroelastic Response of a Rigid Wing Supported by Nonlinear Springs," *Journal of Aircraft*, Vol. 23, No. 4, July-August 1998, pp. 616-622.

[10] Prazenica, R.J., "Wavelet-Based Volterra Series Representations of Nonlinear Dynamical Systems", Ph.D. Dissertation, University of Florida, Gainesville, FL, 2002.

[11] Prazenica, R.J., Lind, R., and Kurdila, A.J., "Uncertainty Estimation from Volterra Kernels for Robust Flutter Analysis," *Journal of Guidance, Control, and Dynamics*, in review.

[12] Reischel, P., "Prediction of Unsteady Aerodynamic Forces via Nonlinear Kernel Identification," *International Forum on Aeroelasticity and Structural Dynamics*, 1999.

[13] Rugh, W.J., *Nonlinear System Theory: The Volterra-Wiener Approach*, John Wiley & Sons, 1980.

[14] Schetzen, M., *The Volterra and Wiener Theories of Nonlinear Systems*, John Wiley & Sons, 1980.

[15] Silva, W., "Application of Nonlinear Systems Theory to Transonic Unsteady Aerodynamic Responses," *Journal of Aircraft*, Vol. 30, No. 5, 1993, pp. 660-668.

[16] Strganac, T.W., Ko, J., Thompson, D.E. and Kurdila, A.J., "Identification and Control of Limit Cycle Oscillations in Aeroelastic System," *Journal of Guidance, Control, and Dynamics*, Vol. 23, No. 6, November-December 2000, pp. 1127-1133.

[17] Wemhoff, E., Packard, A. and Poolla, K., "On the Identification of Nonlinear Maps in a General Interconnected System," *Proceedings of the American Control Conference*, June 1999, pp. 3456-3461.

[18] Wolodkin, G., Rangan, S. and Poolla, K., "An LFT Approach to Parameter Estimation," *Proceedings of the American Control Conference*, June 1997, pp. 2088-2092.